RESEARCH ARTICLE | DECEMBER 09 2024

Correlated photoluminescence blinking phenomenon on InGaN/GaN nanopillar structures

K. Oikawa ; K. Okamoto ; M. Funato ; Y. Kawakami ; R. Micheletto

Appl. Phys. Lett. 125, 243501 (2024)
https://doi.org/10.1063/5.0234331
CHORUS

Applied Physics Letters ARTICLE pubs.aip.org/aip/apl

Correlated photoluminescence blinking phenomenon on InGaN/GaN nanopillar structures

Cite as: Appl. Phys. Lett. **125**, 243501 (2024); doi: 10.1063/5.0234331
Submitted: 21 August 2024 · Accepted: 26 October 2024 ·
Published Online: 9 December 2024

View Online Export Citation CrossMark

K. Oikawa,[1,a] K. Okamoto,[2] M. Funato,[3] Y. Kawakami,[3] and R. Micheletto[1,a]

AFFILIATIONS

[1]Department of Materials System Science, Yokohama City University, 22-2, Seto Kanazawa-ku, Yokohama, 236-0027 Kanagawa, Japan
[2]Department of Physics and Electronics, Osaka Metropolitan University, 1-1 Gakuen-cho, Nakaku, Sakai, Osaka 599-8531, Japan
[3]Department of Electronic Science and Engineering, Kyoto University, Kyoto 615-8510, Japan

[a]**Authors to whom correspondence should be addressed:** n235301d@yokohama-cu.ac.jp and ruggero@yokohama-cu.ac.jp

ABSTRACT

Light-emitting devices that take advantage of the wide bandgap characteristics of InGaN/GaN are widely used in the industry. However, inhomogeneities have been reported in their photoluminescence (PL) mapping at the nanometer and submicrometer scale, even in samples of high crystal quality. In addition, a blinking phenomenon (time variation of PL intensity) under photoexcitation has been reported in relation to these inhomogeneities. The reason why this blinking phenomenon occurs is still unclear; it has been observed in quantum dots and other single and multilayer quantum well structures. Nevertheless, there are very few publications on nanopillar InGaN quantum well samples, which are the focus of this research. Here, we report and analyze the behavior of the blinking phenomena on a nanopillar sample. We noticed that the blinking of the pillars is somehow synchronized on a long timescale among several spatially separated nanopillars. We demonstrated that the synchronization is not due to random intensity fluctuations. We suggest instead that the synchronization is caused by a nonlinear response of the quantum wells to the UV source. In other words, when the stimulation intensity surpasses a certain value, it triggers an ON/OFF state switch in the PL of some of the pillars. Even if preliminary, our study helps to provide clues to understanding the mechanism of the occurrence of the blink phenomenon.

In recent years, InGaN/GaN-based high-efficiency blue light-emitting diodes (LEDs) and laser diodes (LDs) have been commercialized.[1–3] InGaN/GaN samples of practical quality have photoluminescence (PL) mapping known to be inhomogeneous.[4–6] These inhomogeneities in PL intensity have also been reported in measurements using SNOMs, which allow nanoscale measurements in the wavelength region beyond the diffraction limit, which allows submicrometer-scale measurements.[7–12] One of the causes of this inhomogeneity in PL intensity is the presence of numerous threading dislocations (TDs) due to the mismatch of lattice constants between GaN and sapphire, which is the growth substrate, and the phase separation between emitting and non-emitting regions. It has also been reported that quantum confined Stark effect (QCSE) can form PL inhomogeneities.[13] The explanation that associates these PL inhomogeneities with carrier localization as the reason for the efficient PL of InGaN layers has a certain validity when considered in conjunction with the experimental results of carrier dynamics (diffusion length) measurements. The efficiency here is the internal quantum efficiency, which is expressed by the following equation:

$$\eta_{int} = \frac{\kappa_{rad}}{\kappa_{rad} + \kappa_{non}}. \quad (1)$$

Here, κ_{rad} and κ_{non} are the radiative and non-radiative recombination rates, respectively. Overall, these points require a more detailed study of the luminescence properties of InGaN/GaN.

The observation of a blinking phenomenon, in which the luminescence intensity changes with time, has been reported on InGaN/GaN samples.[14–16] Previous studies related to the blinking phenomenon in nitride semiconductor samples have reported blinking emission in bulk with a single quantum well (SQW)[14,15] and cluster samples (1–2 μm multi quantum wells).[16] In the reports of these previous studies, the comparison with the telegraphed blinking phenomenon, which

has been reported in many quantum dot (QD) samples, such as CdSe/CdS/ZnS,[17] has been discussed as to whether the process is caused by a similar mechanism or whether other mechanisms exist. In addition, blinking phenomena have been reported in the nanopillar samples covered in this study, but the content of these reports is limited to the discovery of the phenomena.[18,19] The specific purpose of this study is to provide insight into the relationship between the blinking phenomenon and sample structure by comparing the behavior of blinking in nanopillar grid samples with that of samples with other structures. Here, time series data were analyzed by time-resolved PL mapping measurements using optical excitation for a SQW nanopillar sample (nanopillars are placed on a 30 × 30 grid),[20] which is different from sample structures introduced in previous studies on the blinking phenomenon. The blinking phenomenon was also observed in several nanopillars on the grid sample, and cross correlation analysis was performed for these blinking nanopillars. As a result, we found that the cross correlation coefficient was high at some points among spatially separated blinking pillars, and that their PL intensity was switching from ON/OFF states in a synchronized manner at those nanopillars. Furthermore, we confirmed that the probability distribution of the ON/OFF time interval of the PL intensity signal of the blinking nanopillars is a curve in a one-logarithmic graph. This result is different from the quantum jump model,[21–24] which targets the onset process of the blinking phenomenon in QDs, and is similar to the analysis reported for bulk samples with a SQW structure.

The sample we studied was a sapphire substrate (0001) with a lower growth GaN layer, on top of which was a 3 nm InGaN active layer and a 10 nm GaN cap layer prepared by metal–organic chemical vapor deposition (MOCVD) with an Indium density of the active layer InGaN of 25%. Nanopillars of 0.5–2 μm in diameter with a thickness of about 150 nm were fabricated by masking and exposure using electron beam lithography techniques followed by etching (CAIBE) (30 × 30 grid, overall grid size is about 25 × 25 μm^2). In this fashion, each nanopillar results in having an identical SQW structure. The sample was photo-excited and the PL intensity was imaged by a fluorescence microscope and a CCD camera. With a test on polycarbonate, we verified that the UV lamp XY profile is even and homogeneous within 3%. The measurements were conducted at room temperature. The sample PL obtained is shown in Fig. 1(a). The image is composed of 400 × 400 pixels, and the actual size is about 40 × 40 μm^2. Each round shape represents a pillar, where each of them is separated by the other by approximately the same submicrometer meter distances as depicted schematically in Fig. 1(b). The RGB values of the measured data from the CCD were averaged and grayscaled to obtain the intensity value $I(x, y, t)$ for each frame. We verified that each blinking pillar has one single blinking center, so there is no point in plotting the map at high resolution. Thus, spatial compression was performed through downsampling, that is, reducing the image from 400 × 400 to 80 × 80. This is done by simply discarding pixels, without altering in anyway the actual time-profile of the PL. A pillar is now represented by a single pixel. In this way, processing is faster and mathematical treatment becomes easier since the identification of the pillar's location is straightforward and unique. The time average of optical intensity was calculated for each pixel, and the mapped values are shown in Fig. 2(a) (80 pixels × 80 pixels). The actual image size is about 40 × 40 μm^2. The size of the pillar's array is approximately and 25 × 25 μm^2, as in Fig. 1(a). Also shown in Fig. 2(b) is the calculated and mapped standard deviation value of the optical intensity for each pixel over all time.

$$\overline{I(x,y)} = \frac{1}{n}\sum_{t=0}^{n} I(x,y,t), \tag{2}$$

$$S(x,y) = \sqrt{\frac{1}{n}\sum_{t=0}^{n}\{I(x,y,t) - \overline{I(x,y)}\}^2}. \tag{3}$$

When the value of this standard deviation is high, it indicated that a particular pixel has a large temporal variation of optical intensity, thus it is probably a blinking point. Figures 2(a) and 2(b) represent the optical intensity and the corresponding standard deviation after 30 s of duration, values were normalized to one. Figures 2(c) and 2(d) show the histograms of the mean and the standard deviation values of the same optical intensity. The last figure clearly shows that very few pixels have high optical standard deviation. These are the most visible blinking points. Other the pixels have minor standard deviation, this means that the sample PL emission is affected by low values of optical instabilities, and few of them show evident blinking.

We now focus on those localized areas where the blinking is very strong and evident, that is, the tail of the histogram of Fig. 2(d). For

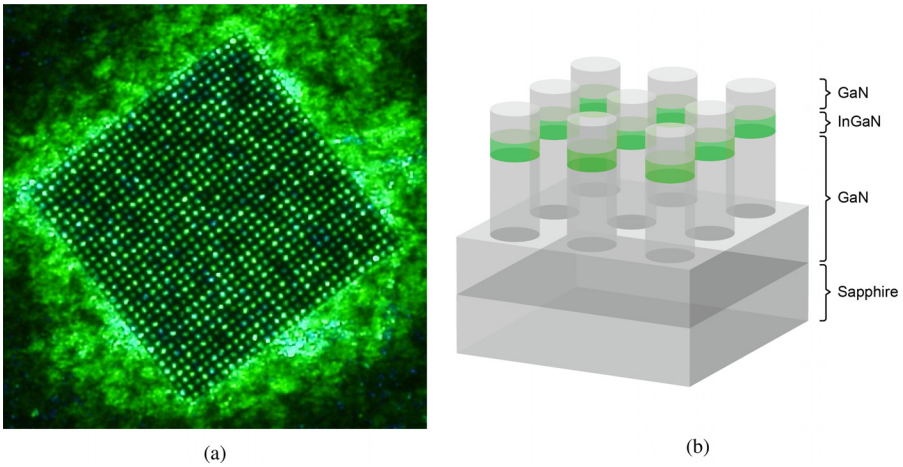

(a) (b)

FIG. 1. (a) Observation of nanopillars using a fluorescence microscope. Nanopillars emitting light and nanopillars quenching light can be seen. (b) Schematic diagram of the InGaN/GaN sample structure.

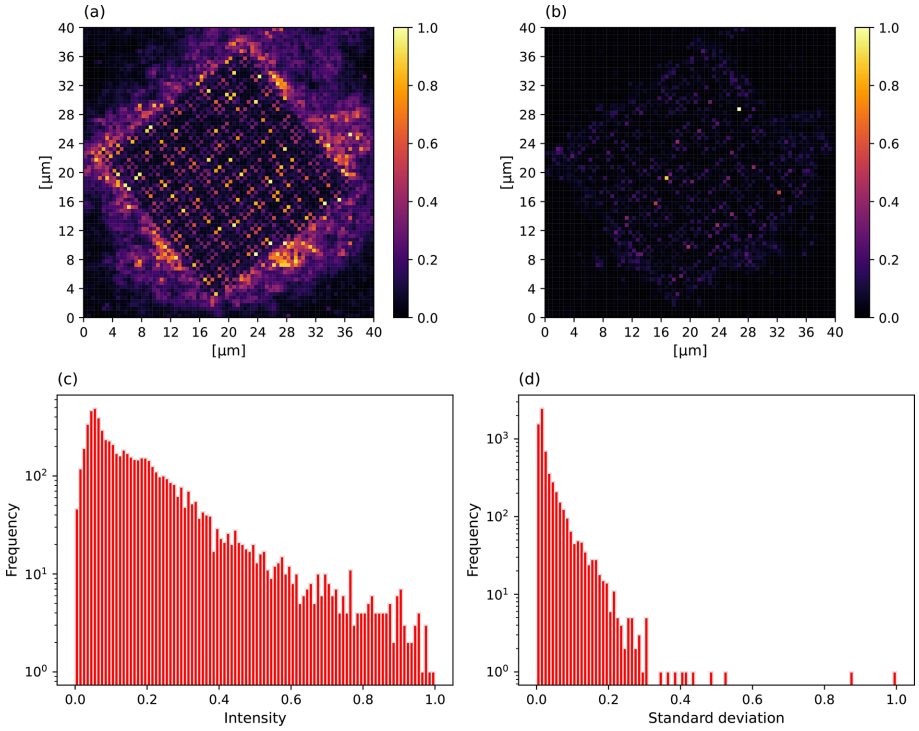

FIG. 2. (a) Map of time average optical intensity values after resizing by linear interpolation (the recording was done for a duration of 30 s, 7.5 measurement per second for a total of 225 samples for each pixel). (b) Map of time standard deviation obtained in the same way. The two maps identify points of higher change in optical intensity (blinking). (c) The distribution of the time averaged optical intensity values, notice that the vertical axis (frequency) is reported in log scale. (d) The distribution of optical intensity standard deviation, the vertical axis (frequency) is in log scale.

example, Fig. 3(b-1) plots the time series signal of optical intensity at the point with the highest standard deviation, indicating a type of blinking called "telegraphic"; chaotic blinking with multiple intensity levels has also been reported for bulk samples with a SQW structure of InGaN/GaN. However, in our nanopillar samples, the blinking is found to be dominated by two states blinking. The sample exhibits few evident blinking points that appear to switch ON and OFF at random moments. To investigate if there is any correlation between the switching, we studied the cross correlation coefficients (CCCs). We have chosen as a reference the point with the highest time standard deviation and mapped that cross correlation with the time-series of all the other pixels and we obtained the map in Fig. 3(a). Highly correlated blinking regions appear to be located in distant pillars, the red dots of Fig. 3(a). The time series profile corresponding to four prominent highly correlated locations are plotted in Figs. 3(b-1)–3(b-4), in these plots the time correlation is evident. Notably, the time series in (b-4) is located on an adjacent pixel of (b-1), that is, it is strongly influenced by the blinking pillar in (b-1). The calculation of the correlation was done accordingly as follows:

$$CCCs(x,y) = \frac{\sum_{t=0}^{n}\left\{I(x_{ref},y_{ref},t) - \overline{I(x_{ref},y_{ref})}\right\}\sum_{t=0}^{n}\left\{I(x,y,t) - \overline{I(x,y)}\right\}}{\sqrt{\sum_{t=0}^{n}\left\{I(x_{ref},y_{ref},t) - \overline{I(x_{ref},y_{ref})}\right\}^2}\sqrt{\sum_{t=0}^{n}\left\{I(x,y,t) - \overline{I(x,y)}\right\}^2}}. \quad (4)$$

In this, I_{ref} is the signal of an arbitrary blinking point used as a reference. As described above, in our algorithms, the blinking point with the highest standard deviation was automatically picked as the reference. Then, the maps were constructed by calculating the cross correlation coefficient of all pixels with respect to these reference points (obviously, the cross correlation coefficient between the reference and itself comes out to be 1.0, thus each correlation map has a point at CCC = 1). Pairs of blinking points with higher cross correlation coefficients have higher temporal similarity, regardless of their intensity. The lamp intensity profile at the sample plane may have some spatially correlated regions (because the Hg lamp is a discharge lamp), so to avoid any doubt, using a setup under the same conditions as the experiments with InGaN, we run our correlation algorithm on a control fluorescent sample (1 mm thick polycarbonate sample) and found uniform PL maps and no time correlation artifacts (<0.03). As mentioned above, the four points with the highest CCCs are plotted in Figs. 3(b-1)–3(b-4). The CCCs were 1.0, 0.76, 0.62, and 0.60, respectively (positive correlation for each). In the plot it can be seen that the optical intensity drops almost simultaneously at around 11 s, it remains OFF for about 6 s, and then turns back ON almost at the same

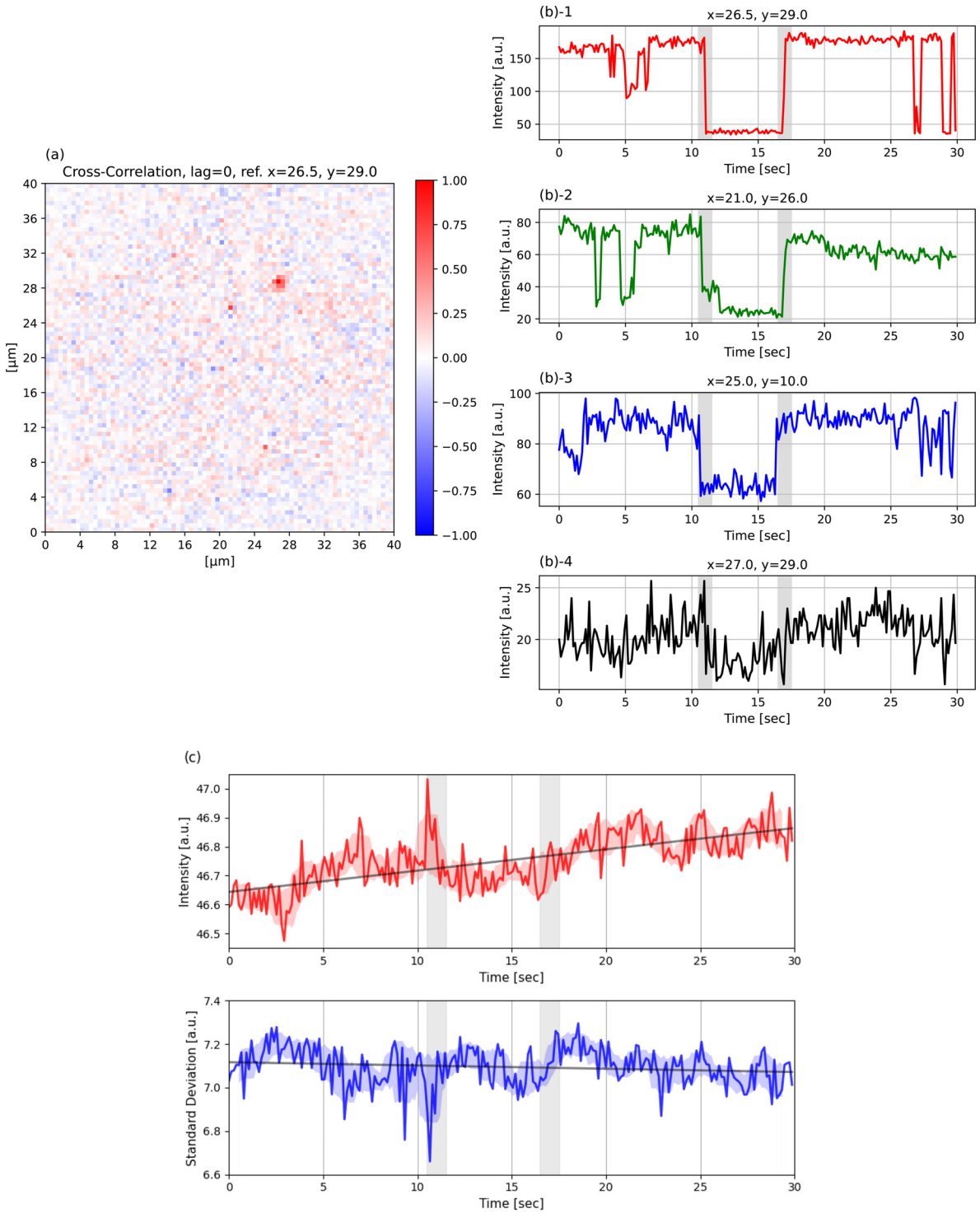

FIG. 3. (a) Cross-correlation coefficient map with the pixel with the largest time standard deviation value as the reference point. The correlation is calculated with null time-lag. Red locations indicate positive correlations and blue locations indicate negative correlations. (b) The time series of optical intensity data are shown in order of the highest cross correlation coefficient. (b-1) is the reference point and has a cross correlation coefficient of 1. On the top of each panel are indicated the coordinates of the relative pixel in (a). (c) The mean value of optical intensity in each frame is plotted in the upper panel. The standard deviation values of optical intensity in each frame are plotted in the lower panel.

moment again at around 17 s. We have already reported a long-period PL intensity change in bulk InGaN/GaN as a "memory effect."[25] It causes PL intensity changes across the entire sample, in other words, it is a phenomenon that acts as a trigger for blinking at any location in the plane. We wanted to verify if there was some global optical phenomenon driving these four pixel synchronizations, so in Fig. 3 we report the mean (c) and standard deviation (d) values of the optical intensity for all pixels (the entire image). The region filled with each color (light red and blue) is obtained by calculating the simple moving average of the last nine frames and calculating the single standard deviation for the upper and lower limits (Bollinger Bands). This global intensity is representing the mercury-xenon light's (Olympus, USH-1030L) total emission that excites the sample PL for the complete duration of the recording. Noticeably, at 11 s, we have a global maximum (minimum for the standard deviation) of this time series. This corresponds to the state switch in the pillars reported in Fig. 3. Intriguingly it is presumably this global fluctuation that induces the observed telegraphic jump of optical emission. As reported above, the correlated ON/OFF switch happens in only some of the pillars, not in all them. This indicates that the three pillars in the figure show a prominent nonlinear sensitivity to the optical power inducing the PL. In other words, this suggests that when the stimulation intensity surpasses a certain value, it triggers a state switch in the PL of the pillars with similar characteristics. In fact, other pillars show an evident state switch at the same moment. In Fig. 4(a), we show a standard deviation analysis similar to that in Fig. 2(b) to map the optical intensity changes within the specific time window between 10 and 12 s, when the mercury-xenon light peak was observed. This map helped us to identify 4 other pillars with a larger standard deviation within that time window. In Fig. 4(b), the complete optical intensity profiles of the same pixels in Fig. 3 are shown.

To better understand the nature of the blinking phenomena on the pillars, an histogram of the ON/OFF intervals was plotted for the entire image in Fig. 5 and for the entire 30 s duration of the experiment. The ON (or OFF) duration time was calculated for each pixel by setting a threshold to define the ON and OFF regions. In a logarithmic scale, according to the quantum jump model,[21–24] we should expect a linear profile, instead the results were different from that predicted by the model. This result suggests that the blinking phenomenon in our nanopillar sample is caused by a non-Poisson process. We should also consider if the synchronous rise of pillar's intensity shown in Figs. 3(b-1)–3(b-4) could be just a random coincidence. In other words, we question if the apparent synchronization in the four points happened by chance. We estimate that the number of actively blinking nanopillars is of about 90, the other 810 pillars appear to have a stable luminosity. For those 90 blinking pixels, using a time-series analysis, we estimated an average number of "blinks" per 30 s of recording. In other words, the average number of sudden intensity changes from OFF to

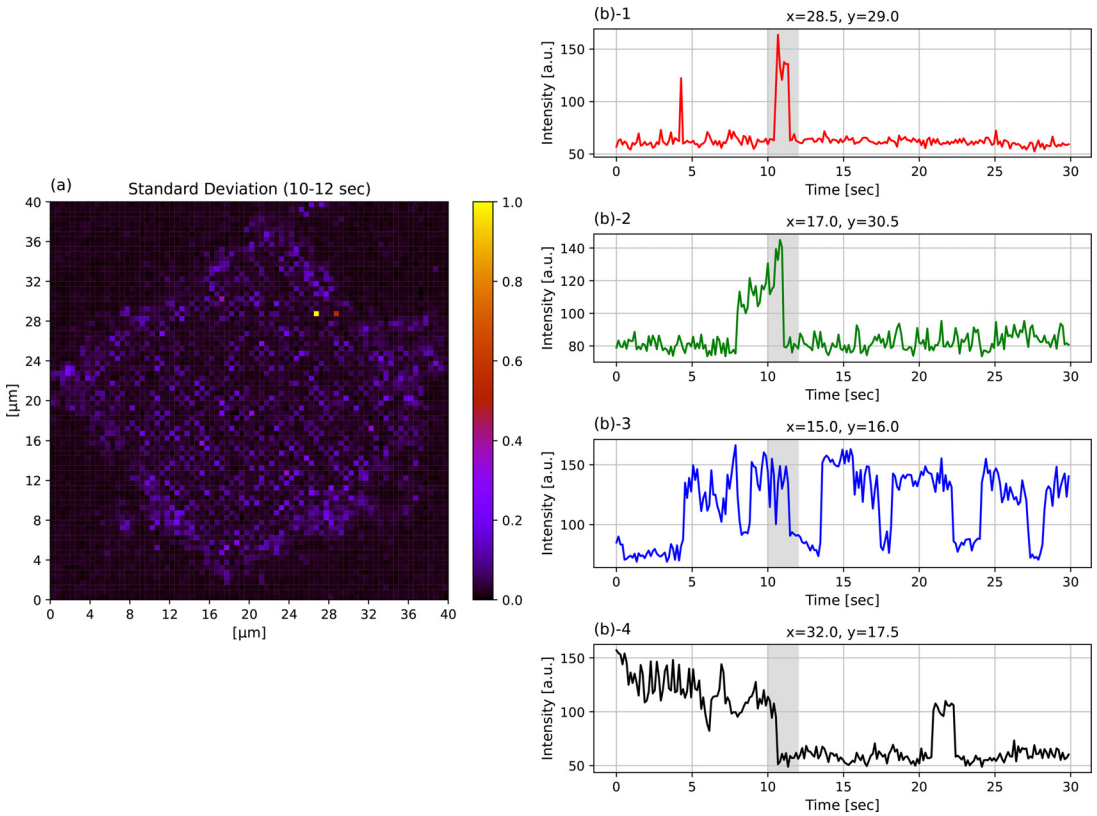

FIG. 4. (a) The standard deviation map corresponding to the 10–12 s interval, when the mercury-xenon light intensity had a peak. It is this higher stimulation intensity peak that presumably caused the synchronization of the blinking pillars reported in Fig. 3(b).

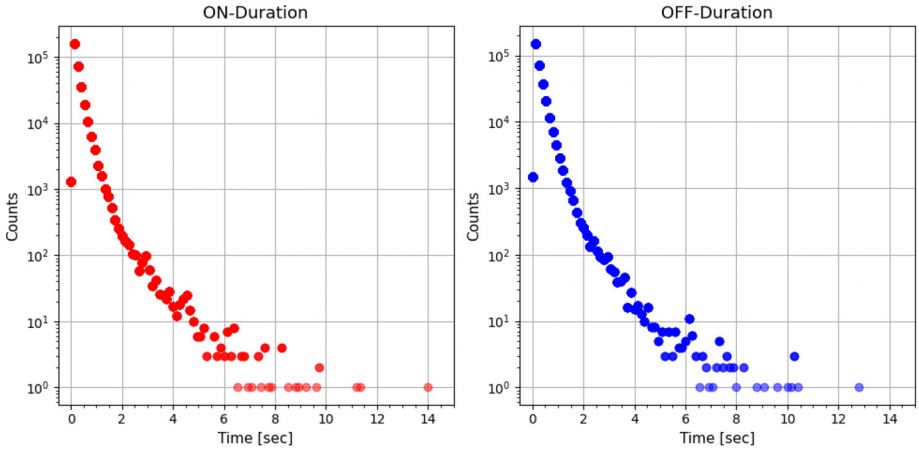

FIG. 5. Histograms of optical intensity intervals (ON, OFF state duration). The vertical axis is in logarithmic scale.

ON (or vice versa) results to be about 5 in the entire recordings, for all the blinking pillars. Since we have 225 samples for each recording, if we hypothesize that the ON/OFF switch happens at random, the probability P_{off} to have a transition from an ON state to OFF (or vice versa) is on average $P_{on/off} = 5/225$ and since we have only 90 blinking regions and considering that $90 * P_{on} \approx 2$, on average, only two pillars should appear to change state in a synchronized fashion. Moreover, in our recording of Figs. 3(b-1)–3(b-4) not only the ON/OFF events are synchronized but also the duration of the state appears to coincide. Again, this should happen by chance with the same probability $P_{off/on} = P_{on/off} = 5/225$. The coincidence of these two events is very rare, $P_{on/off} * P_{off/on} \approx 0.04$, that is, the observed synchronized blinking events reported in Fig. 3 are at 96% confidence not caused by chance (they are not due to random fluctuations). More generally speaking, it is difficult to explain the coincident time interval (duration of the blinking) only by randomness, since the probability distribution is exponential even in our simple two-level model, which is an approximation of the actual optical emission. The ON–OFF intervals result shown in Fig. 5 also suggests that durations of 6 s or longer are very few, thus they are difficult to explain by coincidence only. Without considering cross correlation, slow emission process blinking (long-period blinking) has been reported and discussed in a variety of materials.[25–27]

Again, as shown in Figs. 3(b) and 4(b), optical intensity occurred at almost the same time in several nanopillars, and in Fig. 3(c), changes in values such as image-averaged optical intensity and image-averaged standard deviation at almost the same time suggest the possibility that the state of the entire sample may have migrated. However, it is difficult to indicate a direct causal relationship between these two factors. It can also be seen from Fig. 3(c) that the standard deviation has a correspondent negative peak, so the blinking phenomenon is globally reduced while the total averaged optical intensity increases. Furthermore, we consider that the global changes are due to the GaN growth layer connected to each pillar. In other words, we should suggest a model in which excitons in the growth layer are involved in the dynamics of local luminescence.

Considering the three pillars' recordings in Fig. 3(b), we notice that after the PL emission drops (OFF state), they return to their original state by relaxation over a determined time. This can be thought of as if these pillars have their own intrinsic time of relaxation. This can be thought as an inherent property of similar nanopillars. Inherent properties may be related, for example, to the indium concentration of the nanopillars themselves, as can be seen from the variation in luminescence intensity in Fig. 1(a). Another property that can distinguish each nanopillar can be the presence of trap levels that can change the ON–OFF transition probability. At this stage of the study, it is difficult to directly relate the transition probability to the intrinsic properties of the nanopillar, additional experiments are planned. Specifically, we can interpret the memory effect[25] as a synchronous phenomenon extending on the entire sample, we do not limit what we call "blinking" to a local phenomenon. We currently plan to investigate the exciton diffusion coefficient by controlling the temperature, and conduct experiments on exciton density considering the power density of excitation light and its stability. Moreover, we want to clarify the relationship between the quantum well structure and blinking by wavelength-selective excitation (e.g., switching between 325 and 442 nm). In this paper, all measurements were done at room temperature, in air; however, we plan to measure the blinking in different gas or liquids at different pressures,[28,29] to study how the phenomenon of the correlation will change.

This work was supported by JST SPRING, Japan Grant No. JPMJSP2179. This work was supported by JSPS Grants-in-Aid for the Specially Promoted Research Grant No. JP20H05622.

AUTHOR DECLARATIONS

Conflict of Interest

The authors have no conflicts to disclose.

Author Contributions

K. Oikawa: Conceptualization (lead); Formal analysis (lead); Investigation (lead); Methodology (lead); Visualization (lead); Writing – original draft (lead). **K. Okamoto:** Data curation (equal); Resources (equal); Supervision (supporting); Writing – review & editing (equal). **M. Funato:** Data curation (equal); Resources (equal); Supervision (supporting); Writing – review & editing (equal). **Y. Kawakami:** Data curation (equal); Resources (equal); Supervision (supporting); Writing – review & editing (equal). **R. Micheletto:** Project administration (lead); Supervision (lead); Writing – original draft (equal); Writing – review & editing (lead).

DATA AVAILABILITY

The data that support the findings of this study are available from the corresponding authors upon reasonable request.

REFERENCES

[1]S. Nakamura, "Candela-class high-brightness InGaN/AlGaN double-heterostructure blue-light-emitting diodes," Appl. Phys. Lett. **64**, 1687–1689 (1994).
[2]S. Nakamura, M. Senoh, N. Iwasa, and S. Nagahama, "High-power InGaN single-quantum-well-structure blue and violet light-emitting diodes," Appl. Phys. Lett. **67**, 1868–1870 (1995).
[3]Y. Narukawa, J. Narita, T. Sakamoto, T. Yamada, H. Narimatsu, M. Sano, and T. Mukai, "Recent progress of high efficiency white LEDs," Phys. Status Solidi A **204**, 2087–2093 (2007).
[4]S. F. Chichibu, A. Uedono, T. Onuma, B. A. Haskell, A. Chakraborty, T. Koyama, P. T. Fini, S. Keller, S. P. DenBaars, J. S. Speck *et al.*, "Origin of defect-insensitive emission probability in In-containing (Al, In, Ga) N alloy semiconductors," Nat. Mater. **5**, 810–816 (2006).
[5]S. Chichibu, T. Azuhata, T. Sota, and S. Nakamura, "Excitonic emissions from hexagonal GaN epitaxial layers," J. Appl. Phys. **79**, 2784–2786 (1996).
[6]Y. Narukawa, Y. Kawakami, M. Funato, S. Fujita, S. Fujita, and S. Nakamura, "Role of self-formed InGaN quantum dots for exciton localization in the purple laser diode emitting at 420 nm," Appl. Phys. Lett. **70**, 981–983 (1997).
[7]Y. Kawakami, A. Kaneta, K. Omae, A. Shikanai, K. Okamoto, G. Marutsuki, Y. Narukawa, T. Mukai, and S. Fujita, "Recombination dynamics in low-dimensional nitride semiconductors," Phys. Status Solidi B **240**, 337–343 (2003).
[8]A. Kaneta, M. Funato, and Y. Kawakami, "Nanoscopic recombination processes inInGaN/GaN quantum wells emitting violet, blue, and green spectra," Phys. Rev. B **78**, 125317 (2008).
[9]R. Micheletto, M. Allegrini, and Y. Kawakami, "Near-field evidence of local polarized emission centers in InGaN/GaN materials," Appl. Phys. Lett. **95**, 211904 (2009).
[10]K. Oikawa, C. Feldmeier, U. T. Schwarz, Y. Kawakami, and R. Micheletto, "Near-field evidence of local polarized emission centers in InGaN/GaN materials," Opt. Mater. Express **1**, 158–163 (2011).
[11]K. Okamoto, J. Choi, Y. Kawakami, M. Terazima, T. Mukai, and S. Fujita, "Submicron-scale photoluminescence of InGaN/GaN probed by confocal scanning laser microscopy," Jpn. J. Appl. Phys., Part 1 **43**, 839 (2004).
[12]A. Kaneta, K. Okamoto, Y. Kawakami, S. Fujita, G. Marutsuki, Y. Narukawa, and T. Mukai, "Spatial and temporal luminescence dynamics in an InxGa1-xN single quantum well probed by near-field optical microscopy," Appl. Phys. Lett. **81**, 4353–4355 (2002).
[13]T. Takeuchi, S. Sota, M. Katsuragawa, M. Komori, H. Takeuchi, H. Amano, and I. Akasaki, "Quantum-confined Stark effect due to piezoelectric fields in GaInN strained quantum wells," Jpn. J. Appl. Phys., Part 2 **36**, L382 (1997).
[14]R. Micheletto, M. Abiko, A. Kaneta, Y. Kawakami, Y. Narukawa, and T. Mukai, "Observation of optical instabilities in the photoluminescence of InGaN single quantum well," Appl. Phys. Lett. **88**, 061118 (2006).
[15]S. De, A. Layek, A. Raja, A. Kadir, M. R. Gokhale, A. Bhattacharya, S. Dhar, and A. Chowdhury, "Two distinct origins of highly localized luminescent centers within InGaN/GaN quantum-well light-emitting diodes," Adv. Funct. Mater. **21**, 3828–3835 (2011).
[16]T. Aoki, Y. Nishikawa, and M. Kuwata-Gonokami, "Room-temperature random telegraph noise in luminescence from macroscopic InGaN clusters," Appl. Phys. Lett. **78**, 1065–1067 (2001).
[17]S. J. W. Vonk and F. T. Rabouw, "Biexciton blinking in CdSe-based quantum dots," J. Phys. Chem. Lett. **14**, 5353–5361 (2023).
[18]K. Okamoto and Y. Kawakami, "High-efficiency InGaN/GaN light emitters based on nanophotonics and plasmonics," IEEE J. Sel. Top. Quantum Electron. **15**, 1199–1209 (2009).
[19]K. Okamoto, *Highly Enhanced Light Emissions from InGaN/GaN Based on Nanophotonics and Plasmonics* (Springer International Publishing, Cham, 2021), pp. 1–35.
[20]Y. Kawakami, A. Kaneta, L. Su, Y. Zhu, K. Okamoto, M. Funato, A. Kikuchi, and K. Kishino, "Optical properties of InGaN/GaN nanopillars fabricated by postgrowth chemically assisted ion beam etching," J. Appl. Phys. **107**, 023522 (2010).
[21]R. J. Cook and H. J. Kimble, "Possibility of direct observation of quantum jumps," Phys. Rev. Lett. **54**, 1023 (1985).
[22]G. Yuan, D. E. Gómez, N. Kirkwood, K. Boldt, and P. Mulvaney, "Two mechanisms determine quantum dot blinking," ACS Nano **12**, 3397–3405 (2018).
[23]C. Galland, Y. Ghosh, A. Steinbrück, M. Sykora, J. A. Hollingsworth, V. I. Klimov, and H. Htoon, "Two types of luminescence blinking revealed by spectroelectrochemistry of single quantum dots," Nature **479**, 203–207 (2011).
[24]J. Liu and L. Coolen, "Auger effect in weakly confined nanocrystals," Light Sci. Appl. **12**, 179 (2023).
[25]C. Feldmeier, M. Abiko, U. T. Schwarz, Y. Kawakami, and R. Micheletto, "Transient memory effect in the photoluminescence of InGaN single quantum wells," Opt. Express **17**, 22855–22860 (2009).
[26]B. Kim, I. Kuskovsky, I. P. Herman, D. Li, and G. F. Neumark, "Reversible ultraviolet-induced photoluminescence degradation and enhancement in gan films," J. Appl. Phys. **86**, 2034–2037 (1999).
[27]P. Frantsuzov, M. Kuno, B. Jankó, and R. A. Marcus, "Universal emission intermittency in quantum dots, nanorods, and nanowires," Nat. Phys. **4**, 519–522 (2008).
[28]T. Tsutsumi, G. Alfieri, Y. Kawakami, and R. Micheletto, "The relation between photoluminescence properties and gas pressure with [0001] InGaN single quantum well systems," Appl. Surf. Sci. **392**, 256–259 (2017).
[29]S. Yoshida, Y. Fujii, G. Alfieri, and R. Micheletto, "The influence of water and ethanol adsorption on the optical blinking in InGaN quantum wells," Semicond. Sci. Technol. **37**, 095009 (2022).